Astrocyte inactivation of the pRb pathway predisposes mice to malignant astrocytoma development that is accelerated by PTEN mutation

Andrew Xiao,[1] Hua Wu,[1] Pier Paolo Pandolfi,[2] David N. Louis,[3] and Terry Van Dyke[1,4]

[1]Department of Biochemistry and Biophysics, University of North Carolina at Chapel Hill, Chapel Hill, North Carolina 27599
[2]Molecular Biology Program and Department of Pathology, Sloan-Kettering Institute, Memorial Sloan-Kettering Cancer Center, New York, New York 10021
[3]Department of Pathology and Neurosurgical Service, Massachusetts General Hospital and Harvard Medical School, Charlestown, Massachusetts 02129
[4]Correspondence: tvdlab@med.unc.edu

Summary

We have inactivated pRb, p107, and p130 in astrocytes by transgenic expression of T_{121} (a truncated SV40 T antigen) under the GFAP promoter. Founder mice died perinatally with extensive expansion of neural precursor and anaplastic astrocyte populations. In astrocytes, aberrant proliferation and extensive apoptosis were induced. Using a conditional allele of T_{121}, early lethality was circumvented, and adult mice developed high-grade astrocytoma, in which regions of decreased apoptosis expressed activated Akt. Indeed, astrocytoma development was accelerated in a *PTEN*$^{+/-}$, but not *p53*$^{+/-}$, background. These studies establish a highly penetrant preclinical model for astrocytoma based on events observed in the human disease and further provide insight into the role of PTEN mutation in astrocytoma progression.

Introduction

Astrocytomas are divided into three grades: astrocytoma (WHO grade II), anaplastic astrocytoma (WHO grade III) and glioblastoma (WHO grade IV) (Maher et al., 2001; Reilly and Jacks, 2001; Louis and Cavenee, 2001). Primarily because of its diffuse nature, there is no effective treatment for astrocytoma, and little is known about the mechanism(s) by which it develops. For example, the susceptible target cell(s) is not clear, cause and effect relationships between genetic lesions and cell/tissue responses are largely undetermined, and the molecular and cellular basis for progression from low- to high-grade malignancy is not understood. Experimental animal models are required to understand the complexities of this disease and to develop reasonable therapies for its treatment.

70% to 80% of human grade III and IV gliomas carry mutations in the pRb pathway, including *INK4a* locus mutation (33%–68%), direct *Rb* inactivation (20%–30%) or CDK4 overexpression (10%–15%) (Henson et al., 1994; Ueki et al., 1996). Within tumors, such mutations are generally mutually exclusive, supporting the idea that these factors function within the same pathway (Ueki et al., 1996). Other genetic alterations common in astrocytoma/glioblastoma include *p53* (30%) and *PTEN* (50%) loss-of-function and EGFR (30%) gain-of-function mutations (Reilly and Jacks, 2001; Louis and Cavenee, 2001; Maher et al., 2001). Given the high frequency with which pRb function is impaired in human astrocytoma, we tested the impact of inactivating this pathway specifically in astrocytes of genetically engineered mice. T_{121}, a truncated SV40 T antigen mutant, was used to dominantly inactivate pRb, p107, and p130 (referred to collectively as Rb_f) in astrocytes. We previously showed that transgenic expression of T_{121} in brain choroid plexus epithelial cells induced aberrant proliferation and apoptosis, predisposing them to tumorigenesis (Symonds et al., 1994; Lu et al., 2001). Here, we test whether astrocytes respond similarly to Rb_f inactivation, whether a defect in this pathway predisposes to astrocytoma, and whether mutations in *p53* or *PTEN* cooperate with Rb_f inactivation in astrocytoma development.

Results

Astrocyte-specific pRb_f inactivation causes widespread brain abnormalities

A transcriptional regulatory fragment from the human glial fibrillary acidic protein (*GFAP*) gene was used to direct T_{121} expres-

SIGNIFICANCE

Astrocytoma, rarely amenable to standard therapies, is the most common primary human brain tumor. Mutations in the pRb pathway (70%–80%) and in PTEN (50%) are common and often concurrent in these tumors. Yet, roles for these pathways in astrocytoma development have not been explored in vivo. We show that pRb pathway inactivation in transgenic mouse astrocytes predisposes to the development of high grade astrocytomas. Mice that further carry a single null *PTEN* allele develop disease with shortened latency, providing evidence that *PTEN* mutation is causal in astrocytoma development, but may require collaborating events. This mouse model provides a tool for understanding astrocytoma development and may also be useful in preclinical testing of therapeutic approaches.

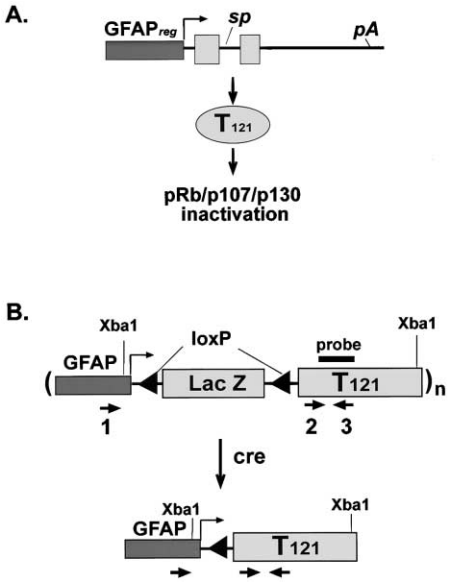

Figure 1. Transgene design

A: In the *GFAP-T$_{121}$* transgene, a 2.2 Kb human GFAP containing transcriptional regulatory signals (dark gray box) was linked to the SV40 early region carrying a deletion of the small t antigen-specific splice signal and a deletion that results in a truncation of large T antigen at aa 121. T$_{121}$ reading frames (light gray boxes), SV40 large T antigen intron (*sp*), and the SV40 early region polyA signal (pA) are indicated. The T$_{121}$ protein binds to and inactivates pRb, p107, and p130. **B:** In the GZT$_{121}$ transgene a LacZ cassette flanked by lox P sites was inserted between GFAP regulatory signals and the T$_{121}$ gene. Due to the stop signals in the LacZ gene, T$_{121}$ expression is not possible until the cassette is deleted by Cre-mediated recombination. When the transgene is integrated as a multicopy head-to-tail array (as is typical), recombination can reduce the original multicopy (n) transgene to a single copy. The probe for Southern hybridization and primers for PCR assays to detect the Cre-mediated deletion are indicated.

sion in transgenic mice (Figure 1A). This fragment has been shown to drive transgene expression within the CNS astrocyte lineage (e.g., Brenner et al., 1994; Holland and Varmus, 1998). Of 13 *TgGFAPT$_{121}$* transgenic founder mice produced, 10 developed severe brain abnormalities (hydrocephalus and/or macrocephaly) and died by postnatal (p) days 7–9 (see Supplemental Table S1 at http://www.cancercell.org/cgi/content/full/1/1/157/DC1). Other organs appeared normal, consistent with the specificity of the GFAP promoter. Similar abnormalities were present in the 6 brains examined. Brains were hypercellular and contained two morphologically distinct abnormal cell populations (Figure 2). One poorly differentiated population was located in the periventricular region of the lateral ventricles and resembled persistent germinal matrix (Figure 2D, e.g., region I and 2E). These cells had small, rounded to angular, densely hyperchromatic nuclei with scant cytoplasm (Figure 2E). A second aberrant cell population was present diffusely throughout the brain (Figure 2D; e.g., region II) and was composed of cells with larger, more irregular, sometimes oval nuclei with vesicular chromatin and occasionally visible small cell processes (Figure 2F), thus resembling developing glial cells and the cells of anaplastic astrocytic neoplasms (Kleihues and Cavenee, 2000).

To investigate cellular origins, brain sections were analyzed for the presence of specific markers. GFAP, a component of the astrocyte intermediate filament, was detected in the diffuse astrocytoma-like cells (Figure 3A), but was absent from the periventricular cells (Figure 3D). Neither population expressed synaptophysin, a marker of mature neurons (not shown). Periventricular cells were characteristic of neural progenitors based on positivity for Tuj-1 and PSA-NCAM (Figures 3C and 3F, respectively) (Doetsch et al., 1997) and the absence of S-100 (glial-specific) and vimentin (glial progenitor-specific) (not shown). Tuj-1 and PSA-NCAM were not expressed in the anaplastic GFAP-positive cells (not shown), consistent with an astrocytic phenotype for these cells.

To determine whether both abnormal cell populations were induced by intrinsic inactivation of the pRb pathway, brain sections were analyzed for T$_{121}$ expression by immunohistochemistry. Consistent with the use of the GFAP promoter to drive transgene expression, T$_{121}$ was expressed in diffuse anaplastic cells (Figure 3B), but not in the majority of primitive periventricular cells (Figure 3E). Colocalization immunofluorescence showed that most T$_{121}$-expressing cells also expressed GFAP, confirming their astrocytic origin (Figures 3G–3J). Since T$_{121}$ was not detected in the abnormal periventricular regions, the mechanism by which these cells are affected is currently unclear. Possible explanations include T$_{121}$ expression at a prior differentiation stage, dedifferentiation of T$_{121}$-expressing astrocytes, or non-cell autonomous effects produced by aberrant astrocytes. Developmental studies will be required to distinguish these possibilities.

Rb$_f$ inactivation induces astrocyte proliferation and apoptosis

We previously demonstrated that pRb$_f$ inactivation by T$_{121}$ expression in choroid plexus epithelial (CPE) cells induced both proliferation and apoptosis. To determine whether similar responses occurred in anaplastic T$_{121}$-expressing astrocytes, proliferation was assessed using immunofluorescence to detect coexpression of T$_{121}$ and PCNA (Figures 4A–4D and 4G). Among the T$_{121}$-positive cells, 32%–38% also expressed PCNA, while only 6%–8% of T$_{121}$-negative cells from the same region expressed PCNA. In a similar location of age-matched nontransgenic brains, $<$1% of the cells were PCNA-positive (Figure 4G). The moderate proliferation increase in T$_{121}$-negative cells of transgenic mice likely indicates the presence of reactive glia responding to extensive brain abnormalities.

To determine the apoptotic rate, TUNEL analysis was performed on age-matched transgenic and nontransgenic brains (Figures 4E, 4F, and 4H). 6% to 7% of the cells in T$_{121}$-expressing regions were apoptotic, while such cells were rarely detected in any region of nontransgenic brains (with the exception of the rostral migratory route [data not shown and Kirschenbaum et al., 1999; Brunjes and Armstrong, 1996]) (Figure 4H). By comparison, 1.7%–2% of the cells were apoptotic in abnormal T$_{121}$-negative periventricular regions (Figure 4H). Thus in astrocytes, as in CPE, pRb$_f$ inactivation induces extensive proliferation and apoptosis.

Inducible astrocyte Rb$_f$ inactivation predisposes adult mice to high grade astrocytoma

Since *TgGFAPT$_{121}$* mice died perinatally, we were unable to determine whether increased astrocyte proliferation and apoptosis could lead to tumorigenesis in adult mice. To address this issue, we generated transgenic mice (*TgGZT$_{121}$*) in which T$_{121}$ expression could be induced by Cre-mediated deletion of

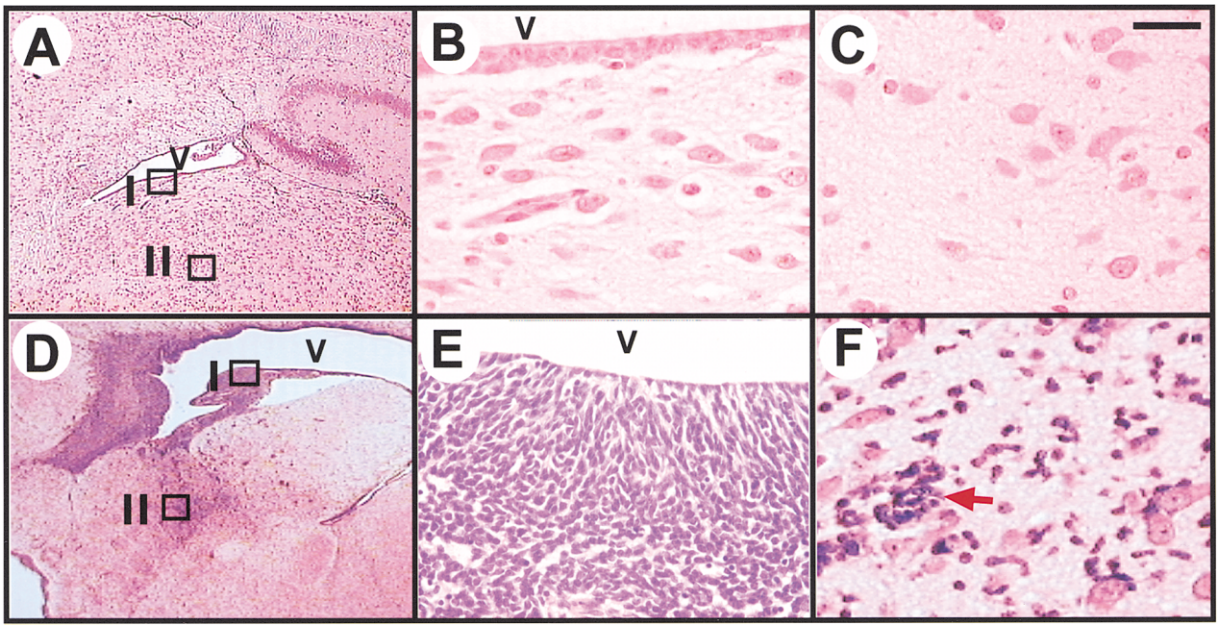

Figure 2. Astrocyte-specific inactivation of the Rb pathway induces extensive brain abnormalities

Representative brain histopathology of the *TgGFAP-T_{121}* transgenic founder mice (**D**–**F**) is shown in comparison to an age-matched nontransgenic control (**A**–**C**) at p7. Boxes indicated in **A** and **D** are shown at high power in the remaining panels; region I in **B** and **E** and region II in **C** and **F**. These views are representative of the observed abnormalities described in the text. Region I is present within a large abnormal periventricular area (compare **A** and **D**, **B** and **E**). Region II is representative of the hypercellularity found diffusely throughout the brain (compare **A** and **D**, **C** and **F**). Perineuronal (**F**, red arrow) and perivascular satellitosis and pathological landmarks of human astrocytoma cells are common in this population. V: lateral ventricle. Bar = 200 μm in **A** and **D**; 15 μm in **B**, **C**, **E** and **F**.

an upstream lac Z reporter/stop signal (Figure 1B). Four independent lines of *TgGZT_{121}* mice were produced and shown to express similar patterns of β-galactosidase in glial-rich regions of the brain, including dentate gyrus, cerebral cortex, and hypothalamus (not shown). As anticipated, *TgGZT_{121}* mice did not express T_{121} in the brain (Figure 5B, panel a) or in other organs (not shown), and they remained normal to at least 17 months of age (Figure 5C and Supplemental Table S1 at http://www.cancercell.org/cgi/content/full/1/1/157/DC1).

Originally, we intended to test whether T_{121} expression could predispose to astrocytoma by somatic introduction of Cre using viral vectors. While this will ultimately prove to be an important strategy, we found that the early lethality observed in founder mice could be circumvented even if Cre was introduced during development. Two independent lines of *TgGZT_{121}* mice were crossed to *Tgβ−actinCre* mice, which express Cre under the β-actin promoter beyond the 64-cell stage (Lewandoski and Martin, 1997). The crosses produced all expected genotypes at normal Mendelian frequencies (data not shown). Furthermore, both Southern hybridization analysis of tail DNA (Figure 5A, left panel) and PCR analysis of brain tissue (Figure 5A, right panel) demonstrated that the lacZ cassette was efficiently deleted in doubly transgenic mice. Southern analysis also showed that recombination facilitated a reduction in the copy number, apparently to a single copy, as expected if the transgene had inserted in a tandem head-to-tail array (Figure 5A, left, compare lanes 2 and 3; Lakso et al., 1996; Lewandoski and Martin, 1997).

Consistent with the specificity of the GFAP promoter associated with the *GZT_{121}* transgene, immunohistochemical analysis revealed that T_{121} was expressed diffusely throughout the brains of compound *TgGZT_{121};Tgβ−actinCre* mice and their *T_{121}* transgene-positive offspring (hereafter referred to as *TgG(ΔZ) T_{121}*). However, levels of expression per cell appeared significantly lower than in *TgGFAPT_{121}* founder mice (Figure 5B, compare panels b and d with c), possibly owing to the reduction in transgene copy number. Surprisingly, despite T_{121} expression, all *TgG(ΔZ)T_{121}* mice (>40) survived beyond the perinatal stage (Supplemental Table S1 and Figure 5C), an effect which could be due to the low levels of T_{121} expressed and/or genetic modifiers introduced by the FVB background of the *Tgβ−actinCre* mice. Analysis of p7 compound mice showed that increased periventricular cellularity was indeed present, but was not as severe as in the *TgGFAPT_{121}* founder mice described above (Figure 5B, compare panels e–g). Reduced severity of this phenotype likely facilitated longer survival. As in *TgGFAPT_{121}* mice, increased cellularity was also observed throughout the p7 brain (e.g., Figure 5B), although mitotic figures and cytological irregularities were less prominent. Beyond 1–3 months of age, *TgG(ΔZ)T_{121}* mice showed signs of morbidity including bulging crania and weight loss. The mice became terminally ill by 5–8 months of age due to the presence of malignant anaplastic astrocytomas (Supplemental Table S1 and Figure 5C).

Of 40 brains examined histologically, all contained moderate to marked increases in cellularity that involved essentially all regions (some regions more markedly hypercellular than others), including the brain stem and cerebellum (compare Figures 6A and 6B). In the cerebral cortex, the infiltration pattern was characteristic of astrocytoma, including perineuronal and perivascular satellitosis (Figures 6C and 6D, respectively) as well as subpial spread (not shown). These cytological and architectural

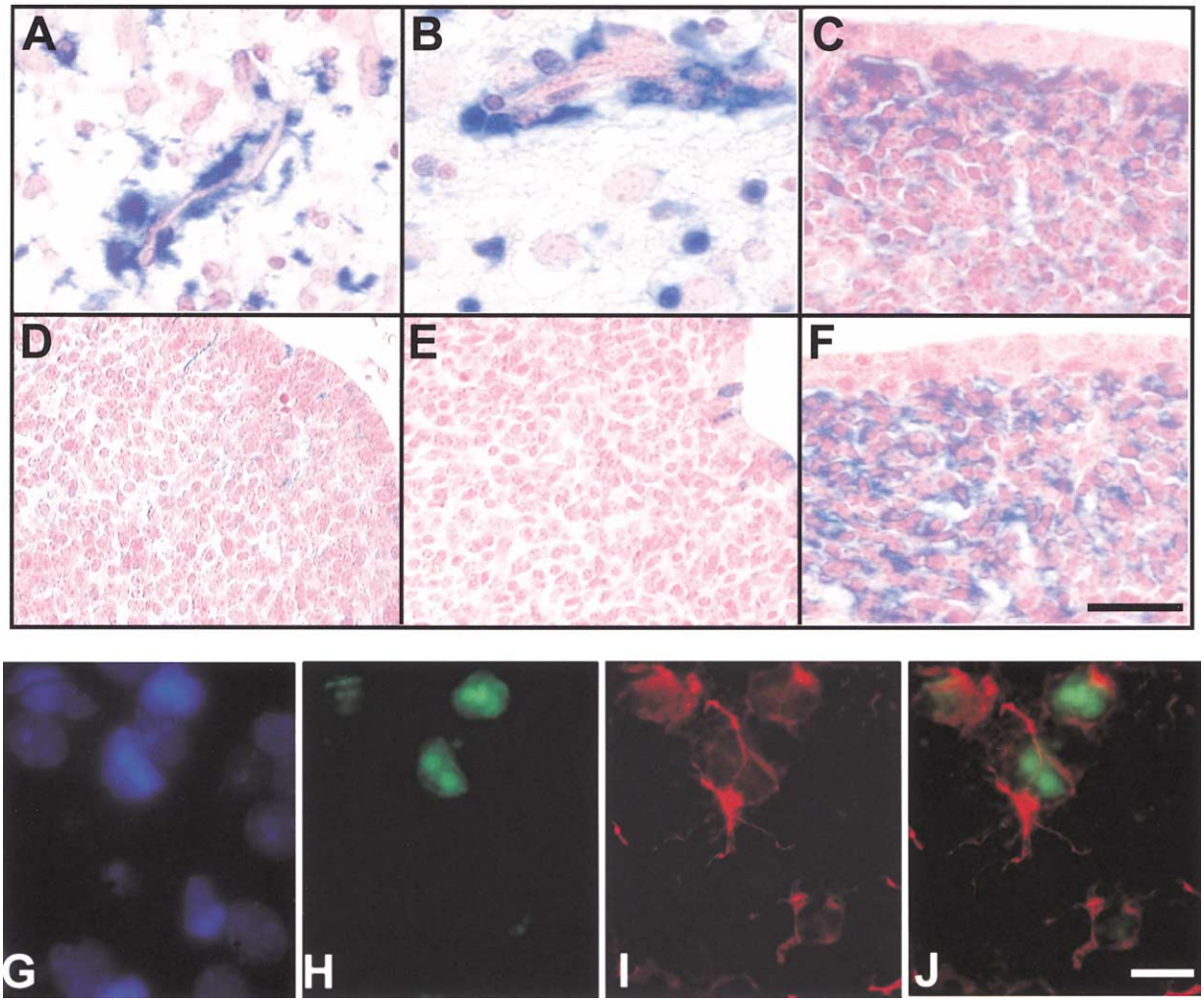

Figure 3. Two distinct brain cell populations are affected

Immunohistochemical assays (**A**–**F**; blue stain = positive) show that diffuse cells (region II, Figure 2) express the astrocytic marker GFAP (**A**) while abnormal periventricular cells (region I, Figure 2) do not (**D**). T_{121} is also expressed in diffuse (**B**) but not periventricular (**E**) cells. Abnormal periventricular cells express the neural precursor markers Tuj1 (**C**) and PSA-NCAM (**F**). Black bar = 20 μM. Immunofluorescence staining of diffuse region II cells shows colocalization of GFAP and T_{121} in most T_{121}-expressing cells (**J**; **H** and **I** merged). T_{121} is detected with a fluorescein conjugated antibody (**H**, green) and GFAP with a rhodamine-conjugated antibody (**I**, red). Nuclei are stained with DAPI (**G**, blue). White bar = 10 μM.

features are consistent with a diffusely infiltrative, malignant astrocytic glioma, with the widespread involvement resembling the extremely infiltrative human condition of gliomatosis cerebri (Kleihues and Cavenee, 2000). The hyperchromatic nuclei, hypercellularity, and mitotic activity would be most consistent with a diagnosis of anaplastic astrocytoma (WHO grade III), with the cells appearing less differentiated than those found in diffuse astrocytomas (grade II), but there is neither the microvascular proliferation nor the necrosis necessary for a diagnosis of glioblastoma (grade IV; Kleihues and Cavenee, 2000). Marker studies are also consistent with these conclusions. Large populations of cells expressed GFAP (Figure 6F), as is often observed in human astrocytomas (Kleihues and Cavenee, 2000). At times, anaplastic cells didn't stain positively for GFAP, or the exact origin of positive signals was difficult to determine. In these cases, staining for S-100 (Figure 6H), a nuclear glial marker (Kimura et al., 1986) along with the absence of synaptophysin, TuJ-1, and PSA-NCAM (not shown), confirmed the astrocytic phenotype of tumor cells. Currently, 44 mice from 2 independent *TgG(ΔZ) T_{121}* lineages have developed astrocytomas (Supplemental Table S1).

Akt kinase is regionally activated during astrocytoma development

The long latency between T_{121} expression (by p7) and the development of life-threatening astrocytomas (generally >100 days) indicates that additional events subsequent to pRb_f inactivation may be required. In human gliomas, EGF and PDGF receptor mediated Ras/MAP kinase and PTEN regulated PI3 kinase/Akt signaling cascades are frequently altered, correlating with tumor progression (Reilly and Jacks, 2001; Louis and Cavenee, 2001; Maher et al., 2001). Thus, we examined tumors for evidence of altered regulation of these pathways.

Activation of Akt kinase by phosphorylation at ser 473 is

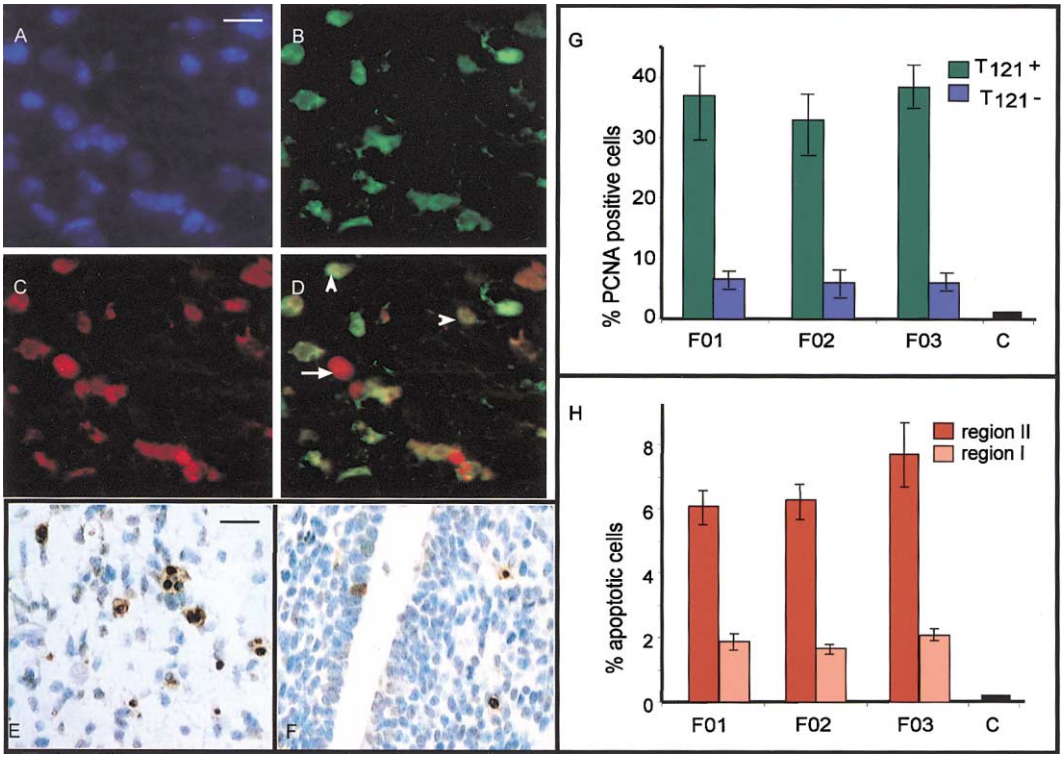

Figure 4. Inactivation of the Rb pathway in astrocytes induces aberrant proliferation and apoptosis

The brains of three independent *TgGFAP-T_{121}* founder mice (F0 1–3, Supplemental Table S1 at http://www.cancercell.org/cgi/content/full/1/1/157/DC1) were analyzed for proliferation (**A**–**D** and **G**) and apoptosis (**E**, **F**, and **H**). Proliferation rates were determined for T_{121}-expressing and nonexpressing cells in regions of the brain that harbored anaplastic cells. Cells were doubly stained for T_{121} (fluorescein/green; **B**) and PCNA (rhodamine/red; **C**) using immunofluorescence. Using the merged image (**D**) the percentage of PCNA positive cells expressing T_{121} (e.g., arrow heads) or not (e.g., arrow) was calculated (**G**). Nuclei were stained with DAPI (blue; **A**). In comparable regions of a p7 nontransgenic control brain, PCNA positive cells were only rarely detected (<1%; C in **G**). The TUNEL assay (positive signal = brown) detected apoptotic cells in regions containing anaplastic astrocytes (**E**) or periventricular neural precursors (**F**). The percentages of apoptotic cells relative to total cells in the regions examined were calculated (**H**). Only rare apoptotic cells (<0.1%) were detected in all comparable regions from a p7 nontransgenic brain. For both proliferation and apoptosis assays, 5 fields (>1000 total cells) were assessed for each brain. Error bars in **G** and **H** indicate the standard deviation among fields. White bar = 20 μM; black bar = 40 μM.

positively regulated by PI3 kinase and PDK1, and negatively regulated by PTEN (Datta et al., 1999 and references therein). Thus, we determined whether Akt was activated in astrocytomas by immunohistochemistry using an antibody specific for P^{Ser473}-Akt. 72% of the astrocytomas (13 of 18; Table 1) demonstrated regional expression of activated Akt (Figure 7A). Such regions were absent from age-matched control *TgGZT_{121}* and *Tgβ−actinCre* mice (data not shown). Akt activation was not a direct effect of T_{121} expression, and likely represents a secondary event in tumorigenesis. Activated Akt was undetectable in young *TgG(ΔZ)T_{121}* brains (3 of 3 mice tested at p7–10; e.g., Figure 7I) and in *TgGFAPT_{121}* founder brains (5 of 5 mice tested, p7–9), despite widespread expression of T_{121} (Figure 7J). Furthermore, when mice were terminally ill, Akt was activated regionally (e.g., compare Figures 7A and 7E from the same brain), while T_{121} was expressed throughout the brain (Figures 7B and 7F).

To confirm the specificity of immunohistochemical assays, immunoblotting was used to assess Akt and P^{Ser473}-Akt expression in primary astrocytes from *TgGZT_{121}* control and *TgG(ΔZ)T_{121}* astrocytoma-containing brains. Consistent with the immunohistochemical results, most tumor cell preparations expressed a significantly higher level of phosphorylated Akt compared with cultures from normal control brains, while the overall level of Akt was unchanged (Figure 7K; Table 1).

Akt activation has been shown to protect cells from apoptotic stimuli (Stambolic et al., 1998; Datta et al., 1999 and references therein). Given the high level of astrocyte apoptosis induced by Rb_f inactivation, we performed TUNEL assays to determine whether tumor regions expressing activated Akt showed evidence of altered apoptotic rates. Indeed, the apoptosis level was greatly reduced in Akt active regions compared to surrounding tissue in 3 of 3 mice examined (e.g., compare Figures 7C and 7G). Proliferating astrocytes were present at similar frequencies in regions with and without activated Akt expression (e.g., compare Figures 7D and 7H). Thus, Akt activation may provide a selective advantage to astrocytoma cells initiated by Rb_f inactivation, at least in part by reducing apoptosis.

We also investigated the phosphorylation status of p42/p44 MAP kinase and Erk1 and 2 by immunohistochemistry. In rodents, Erk 1 and 2 are activated by EGF and PDGF receptor/Ras signaling cascades by phosphorylation of Thr183 and Tyr185 (Schlessinger, 2000 and references therein). Of 18 astrocytoma-containing brains examined, only 2 showed evidence of Erk 1,2 phosphorylation; neither expressed activated Akt (Ta-

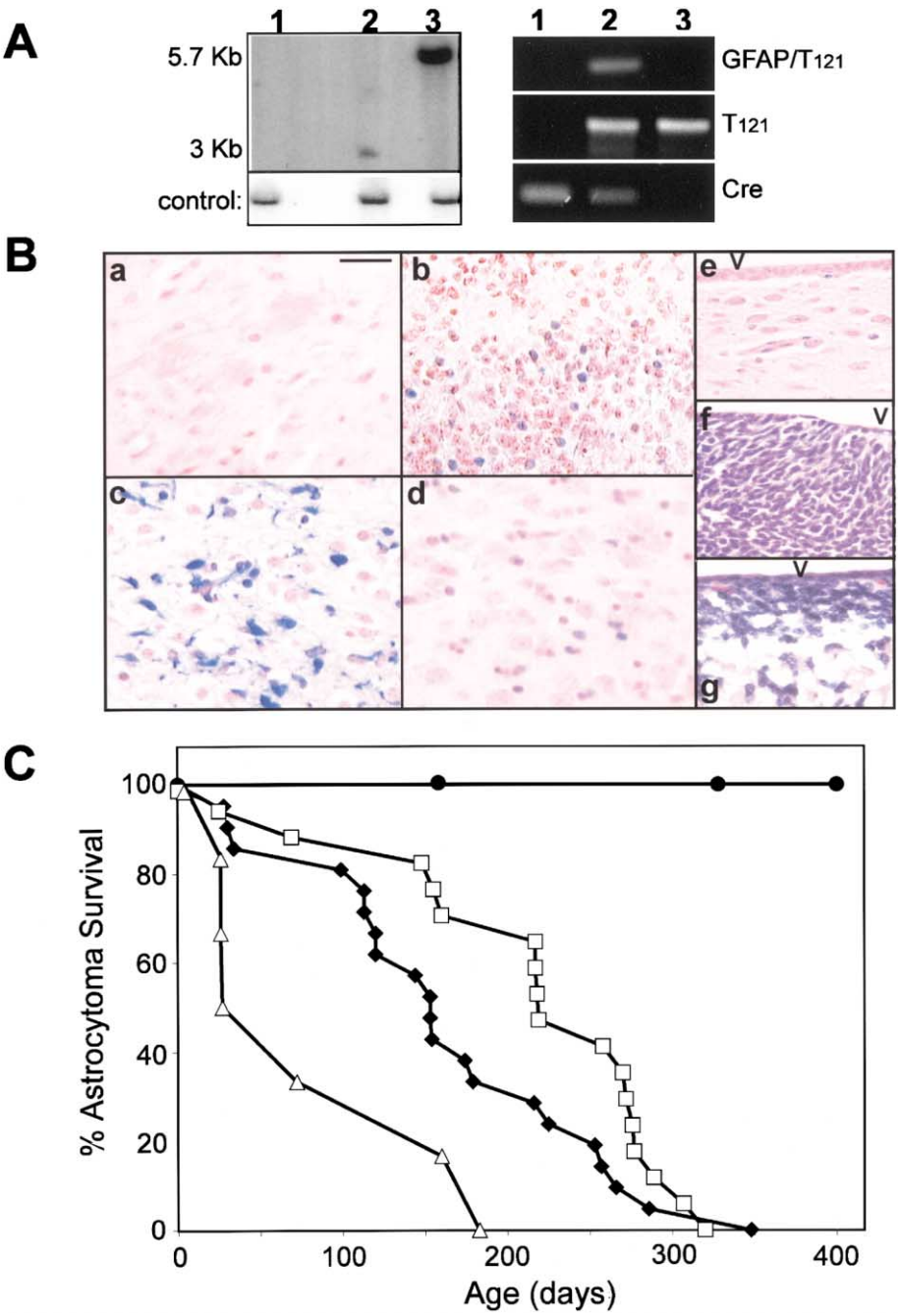

Figure 5. Characterization of *TgG(ΔZ) T_{121}* mice

A: Southern blotting analysis of tail DNA (left panel) indicates that the expected deletion of the *lac Z* cassette along with a reduction in transgene copy number occurred in *TgG(ΔZ) T_{121}* mice (lane 2) compared with *$TgGZT_{121}$* DNA (lane 3). No specific signal was present in control β *-actin Cre* DNA (lane 1). The probe was derived from the *T_{121}* gene (see Figure 1B). All DNAs contained similar signals when hybridized with the *PTEN* control probe. PCR analyses on brain DNA samples (right panel) confirm the removal of the *lacZ* cassette in *TgG(ΔZ)T_{121}* brains (lane 2, primers 1 and 3). Primer sequences 1, 2, and 3 are mapped in Figure 1B. The specificity of the pimers is indicated to the right of the panel. Lanes 1, β *-actin Cre*; lanes 2, *TgG(ΔZ)T_{121}*; lanes 3, *$TgGZT_{121}$*. **B:** Immunohistochemical detection of T_{121} (panels a–d; positive signal = blue) shows T_{121} expression in adult (b) and p7 (d) *TgG(ΔZ) T_{121}* brains, but not in brains of parental adult *$TgGZT_{121}$* (a) or β-actin Cre (not shown) mice. Staining under the same conditions of a p7 *TgGFAP-T_{121}* transgenic founder brain is shown for comparison in panel c. Hypercellularity in the periventricular regions was observed in H&E-stained p7 *TgG(ΔZ) T_{121}* brains (g) compared to a p7 nontransgenic control (e), but was less extensive compared to that of p7 *TgGFAP-T_{121}* founder mice (f). Bar = 20 μM in panels a–d, 30 μM in e–g. **C:** Astrocytoma-free survival of mice is plotted as a function of time. All *TgG(ΔZ) T_{121}* mice died of anaplastic astrocytoma, while all parental uninduced *$TgGZT_{121}$* mice survived beyond 400 days, and none developed astrocytoma (•; n>40). *PTEN*, but not *p53*, mutation cooperates with pRb_f inactivation in the development of astrocytoma. Each data point for *TgG(ΔZ)T_{121}* (◆; n = 21), *TgG(ΔZ)T_{121}; $p53^{+/-}$* (□; n = 17), and *TgG(ΔZ)T_{121} ; $PTEN^{+/-}$* (Δ; n = 6) mice represents the death or sacrifice of a mouse with terminal astrocytoma. Enlarged spleens and lymph nodes were also present in two *TgG(ΔZ)T_{121}; $p53^{+/-}$* mice.

ble 1). Western blotting of primary astrocytes also demonstrated that levels of phosphorylated Erk1 and 2 were similar in normal and tumor astrocytes (Figure 7K, Table 1).

PTEN, but not p53, heterozygosity accelerates astrocytoma tumorigenesis

Inactivating mutations of PTEN, a negative regulator of Akt, occur frequently in high grade human astrocytoma (50%) and thus frequently coexist with mutations in the Rb pathway (see Introduction). Mutation of p53 occurs at a much lower frequency and often appears at early stages (Reilly and Jacks, 2001; Maher et al., 2001; Louis and Cavenee, 2001). In the CP tumor model, p53 deficiency accelerates tumorigenesis by reducing the apoptosis evoked by Rb_f inactivation (Lu et al., 2001; Symonds et al., 1994). Since apoptosis reduction in astrocytomas correlated with Akt activation, we tested the effect of both p53 and PTEN heterozygosity on T_{121}-induced astrocytoma development.

TgG(ΔZ)T_{121} mice heterozygous for null alleles of either gene were generated in standard crosses. Surprisingly, *p53* haplodeficiency did not reduce the latency of astrocytoma ($p > 0.05$, Wilcoxen rank test; Figure 5C). The average lifespan of *TgG(ΔZ)T_{121}* mice was 180 days, while that of *TgG(ΔZ)T_{121};$p53^{+/-}$* mice was 225 days. In most regions of the brain, morphology and cellularity were similar in *TgG(ΔZ)T_{121};$p53^{+/-}$* and *TgG(ΔZ)T_{121}*

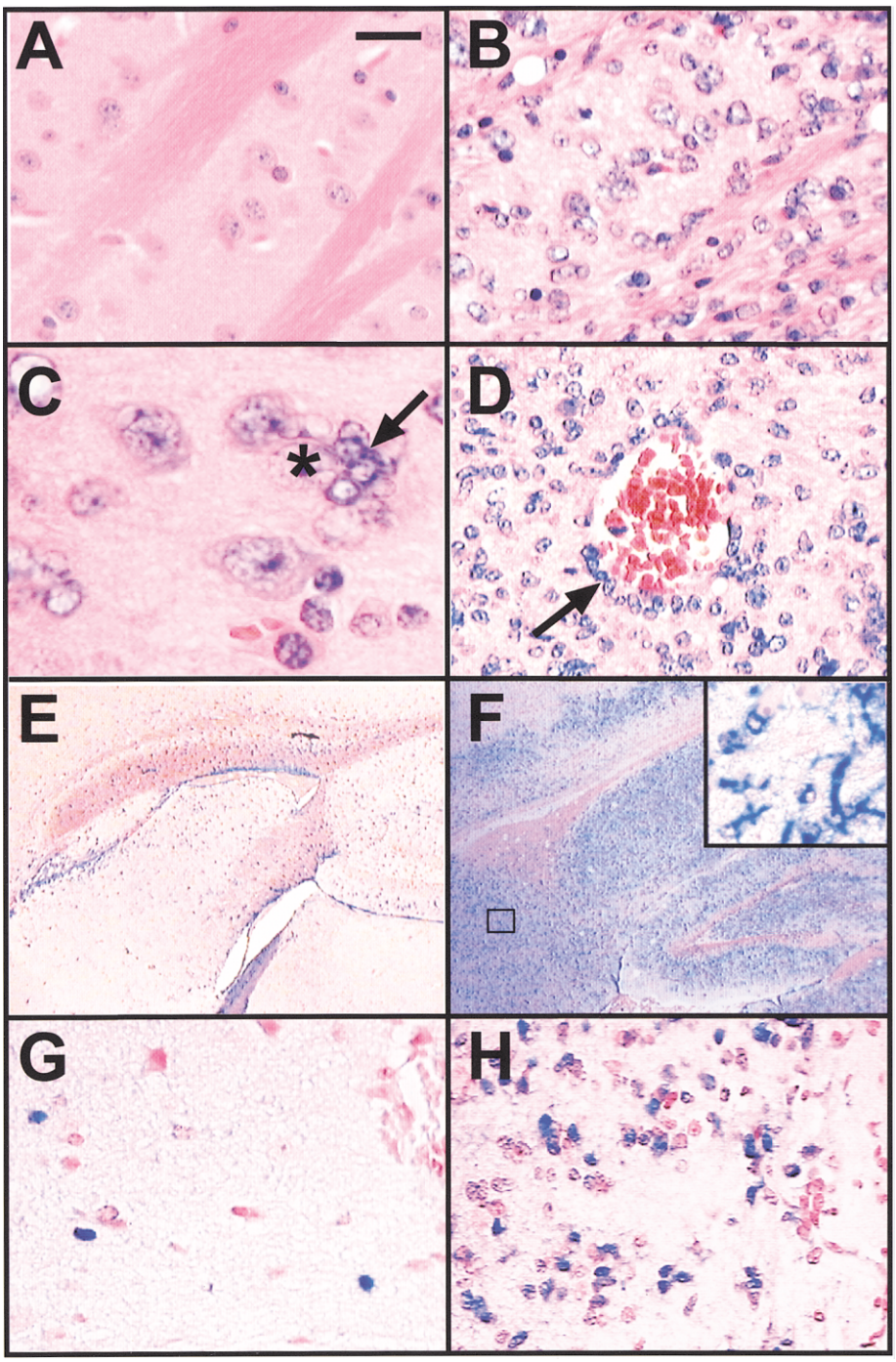

Figure 6. Inactivation of the pRb pathway in astrocytes predisposes to anaplastic astrocytoma

At 5–7 months of age, *TgG(ΔZ) T_{121}* mice develop anaplastic astrocytoma as indicated by histological features common to the human disease (**B**–**D**, **F** and **H**). **A**–**D** are stained with H&E, **E** and **F** with anti-GFAP, and **G** and **H** with anti-S100. Positive immunoreactivity in **E**–**H** is blue. While the brains of *$TgGZT_{121}$* mice are normal at all ages (e.g., 6 months of age; **A**, **E**, and **G**), those of compound mice contain widespread infiltrating anaplastic cells (compare *TgG(ΔZ) T_{121}* brains in **B**, **F**, and **H** with respective controls in **A**, **E**, and **G**). Furthermore, several pathological landmarks of human astrocytoma, such as perineuronal (**C**) and perivascular (**D**) satellitosis, are common. (A neuron is marked by an asterisk in **C**; representative malignant cells are indicated by arrows in **C** and **D**.) Brains with malignancy show widespread GFAP positivity (**F**), including the presence of GFAP-positive cell processes indicative of astrocytoma (**F**, inset). Anaplastic cells are also positive for S100 antigen (**H**). The black bar in **A** represents 20 μM in **A**, **B**, **D**, **G**, **H**, and inset in **F**, 10 μM in **C**, and 200 μM in **E** and **F**.

mice. Of interest, all *$TgG(\Delta Z)T_{121}$;$p53^{+/-}$* mice developed olfactory bulb tumors consisting of giant cells that did not express the astrocyte markers S100 and GFAP (not shown). The origin of these tumors is currently unknown (see Discussion).

The lifespan of *$TgG(\Delta Z)T_{121}$* mice was significantly shortened when mice were heterozygous for a null *PTEN* allele (from an average of 180 days to 72 days, $p < 0.01$, Wilcoxen rank test; Figure 5C). All *$TgG(\Delta Z)T_{121}$;$PTEN^{+/-}$* mice (6 of 6) developed enlarged crania by p7. When mice were terminally ill, brains contained diffuse astrocytic proliferation consistent with a diagnosis of malignant astrocytoma. Brains displayed a diffuse increase in poorly differentiated cells that were cytologically identical to those noted throughout the brains of age-matched *$TgG(\Delta Z)T_{121}$* controls. However, the hypercellularity in *$TgG(\Delta Z)T_{121}$;$PTEN^{+/-}$* brains was more marked, with many cells infiltrating the gray and white matter, including with prominent perineuronal satellitosis and subpial growth. Mitotic activity was also present. However, as with *$TgG(\Delta Z)T_{121}$* mice, neither microvascular proliferation nor necrosis was detected. TUNEL analyses of brains from 17-day-old mice showed apoptosis levels to be reduced

Table 1. Akt and Erk signal transduction pathways in astrocytoma

Genotype	Age(D)[a]	T_{121}	P-Akt (Ser473) IHC[b]	p-Erk(Thr202/Tyr204) IHC[b]	Activation in primary tumor cells[c]	
					p-Akt	p-Erk1,2
$G(\Delta Z)T_{121}^{+/-}$; $Cre^{+/-}$	7*	+(w)	ND	ND		
$Cre^{-/-}$	10*	+(w)	ND	ND		
$Cre^{-/-}$	10*	+(w)	ND	ND		
$Cre^{-/-}$	42	+(w)	BS; HCC	ND	+	—
$Cre^{-/-}$	69	+(w)	Hy	ND		
$Cre^{+/-}$	94	+(w)	HCC; FCC	ND	+	—
$Cre^{+/-}$	99	+(w)	Hy	ND	+	—
$Cre^{+/-}$	113	+(w)	HCC	ND	+	—
$Cre^{+/-}$	113	+(w)	BS; FCC	ND	+	—
$Cre^{+/-}$	120	+(w)	ND	SVZ		
$Cre^{+/-}$	120	+(w)	ND	ND	—	—
$Cre^{+/-}$	144**	+(w)	ND	ND		
$Cre^{+/-}$	153	+(w)	M	ND		
$Cre^{+/-}$	154	+(w)	FCC	ND		
$Cre^{+/-}$	180	+(w)	Hy	ND	+	—
$Cre^{+/-}$	216	+(w)	ND	ND		
$Cre^{+/-}$	225	+(w)	HCC; BS	ND		
$Cre^{+/-}$	253	+(w)	ND	FCC		
$Cre^{+/-}$	266	+(w)	BS	ND		
$Cre^{+/-}$	274	+(w)	HCC; HY; BS	ND		
$Cre^{+/-}$	286	+(w)	Th; M	ND		

[a] All mice except those marked with asterisks (see below) developed life-threatening anaplastic astrocytoma, and showed outward symptoms, e.g., bulged head, and signs of morbidity when sacrificed.
[b] IHC was performed on sections through both hemispheres of each brain. However, step sections sampling the entire brain were not analyzed except for two. Some positive regions might be missed.
[c] Tumor cells were isolated from brains and analyzed at passage two by Western blotting (Experimental Procedures).
* These mice were sacrificed when healthy.
** This mouse died while giving birth; otherwise, it didn't show severe symptoms.
+(w), widespread expression; ND, not detected; IHC, immunohistochemistry; BS, brain stem; HCC, hind cerebral cortex; Hy, hypothalamus; FCC, frontal cerebral cortex; M, midbrain; Th, thalamus; SVZ, subventricular zone; +, upregulated; —, unchanged (compared with WT primary astrocytes). Blank entries: cells were not isolated from these mice.

in *$TgG(\Delta Z)T_{121}$;$PTEN^{+/-}$* compared to *$TgG(\Delta Z)T_{121}$* mice (2.3% versus 4.2%, respectively). However, it is not yet clear whether haploinsufficiency or PTEN inactivation is required for tumor acceleration. Significantly, astrocytomas have not been reported in *$PTEN^{+/-}$* mice, although they develop other tumor types beyond about 5 months of age (Di Cristofano et al., 1998; Podsypanina et al., 1999; Suzuki et al., 1998).

Discussion

Here we demonstrate that inactivation of the pRb pathway in astrocytes induces aberrant proliferation and extensive apoptosis. With 100% penetrance, this condition progresses to malignant anaplastic astrocytoma in adult mice. In more than 70% of these tumors, areas of decreased apoptosis express activated Akt indicative of selective progression. As predicted by this finding, tumorigenesis is accelerated in a *$PTEN^{+/-}$* background. Thus, the highly penetrant *$TgG(\Delta Z)T_{121}$* astrocytoma model resembles the human disease with respect to both the molecular targets and the ensuing pathology. This model should prove useful for further mechanistic elucidation and possibly for preclinical therapeutic testing.

Redundancy in murine pRb tumor suppression

T_{121} inactivates all three pRb-related proteins (pRb, p107, and p130), an activity that requires direct interaction (T antigen amino acids 105–114; Ewen et al., 1989; DeCaprio et al., 1989; Dyson et al., 1989) and an intact J domain (aa 1–82 (Sullivan et al., 2000; Stubdal et al., 1997). Using a mutant T_{121} defective in binding the pRb proteins, we previously showed that this function was required for all T_{121} effects observed in vivo (Saenz-Robles et al., 1994). Interestingly, astrocyte abnormalities are not induced upon inactivation of the *Rb* gene alone, either by conditional deletion (Marino et al., 2000) or by the generation of chimeric mice harboring pRb-deficient cells (Maandag et al., 1994; Williams et al., 1994). Thus, by comparison our results indicate that functional redundancy/compensation occurs among the pRb proteins in mouse astrocyte tumor suppression. Evidence for redundancy among these proteins has also been observed for murine retinal tumor suppression (Robanus-Maandag et al., 1998), in murine development (Cobrinik et al., 1996; Lee et al., 1996), and in mouse embryo fibroblast cell cycle regulation (Sage et al., 2000). Since mutation of the *Rb* gene alone is frequent in human cancers, such compensation may not exist in human cells, or may only be present in limited cell types.

Predisposition to astrocytoma by pRb_f inactivation

In founder transgenic mice expressing high levels of GFAP-directed T_{121} expression, mice died perinatally with extensive expansion of both neural precursor and anaplastic astrocyte populations, with only the latter expressing T_{121}. Using a conditional allele of T_{121} also expressed in astrocytes, early lethality was circumvented, likely because of reduced levels of T_{121} expression and/or modifying effects of a distinct genetic background. In these mice, astrocyte-specific inactivation of the pRb

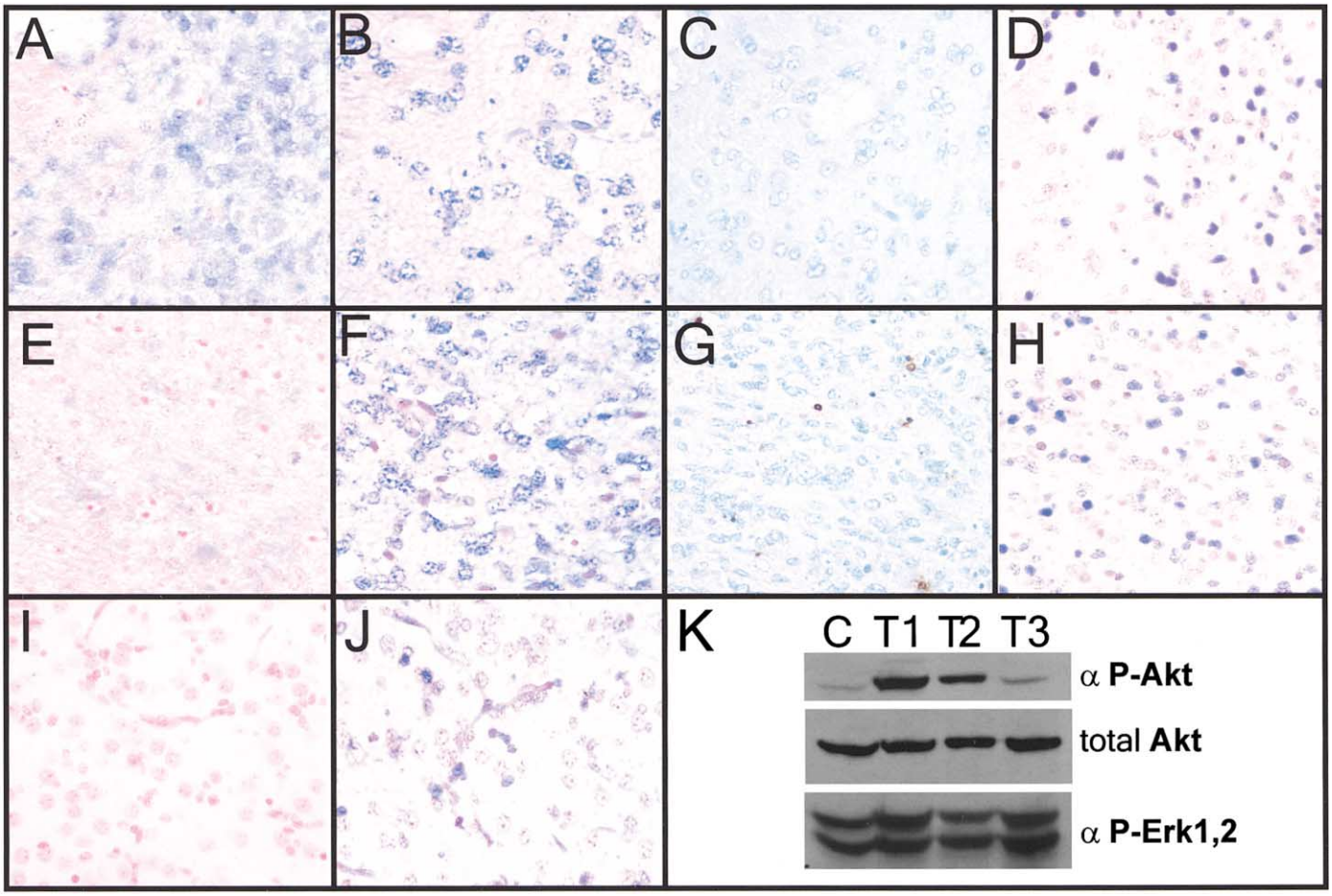

Figure 7. Akt kinase is activated during astrocytomagensis

Fields from the same *TgG(ΔZ)*T_{121} brain with terminal astrocytoma are shown in **A**–**H**. **A**–**D** are from one region, while **E**–**H** are from an adjacent area. Serial sections were analyzed for activated Akt (P-Akt ^{Ser473} level) (**A** and **E**), T_{121} expression (**B** and **F**), and PCNA (**D** and **H**) by IHC (blue staining), and apoptosis by TUNEL (**C** and **G**, brown staining). Anaplastic astrocytes in the region expressing activated Akt (**A**–**D**) are proliferating based on PCNA staining and express similar levels of T_{121}, as do cells in the region not expressing activated Akt (**E**–**H**). However, apoptosis levels are reduced (compare **C** and **G**). Serial sections of a brain from a 7-day-old *TgG(ΔZ)*T_{121} mouse are shown in **I** and **J**. Activated Akt expression was not detected (**I**), although cells in the same region expressed T_{121} (J). Western blotting analysis of primary astrocytes (**K**) also demonstrated that P-Akt ^{Ser473} levels were increased in tumor cells (T 1-2) relative to normal cells (**C**), while the level of total Akt and p-Erk1,2$^{Thy183/Tyr185}$ were unchanged. Tumors (T) 1 and 2 contained regions that were positive for activated Akt by IHC, while such regions were not detected in tumor 3.

proteins predisposed cells to malignant astrocytoma. Although the expansion of neural precursors was diminished in these mice compared with *TgGFAPT*$_{121}$ founders, this population remained abnormally abundant. Whether this property contributes to the development of astrocytoma is not clear. Experiments are underway to determine the role, if any, of such cell-cell interactions in this disease.

We examined the role of pRb_f inactivation in astrocytoma because this pathway is disrupted in nearly all human high-grade astrocytomas (see Introduction). Yet our results show that inactivation of this pathway *can* constitute an initiating event in the development of high-grade astrocytomas. It is possible that stochastic inactivation of this pathway occurs in astrocytes only as a result of selective pressures created by foregoing initiating events. It may also be that tumors initiated by pRb inactivation progress rapidly to high-grade disease. The *TgGZT*$_{121}$ mice, in which pRb inactivation can be induced somatically, will provide an excellent model for exploring these aspects of tumor evolution.

Recent studies have shown that the activation of Ras signaling pathways can predispose to glioblastoma or glioma-like lesions in mice. Somatic delivery of *K-ras*^{G12D} and *Akt* genes together (but not alone) into neural progenitor cells via retroviral vectors induced glioblastoma (Holland et al., 2000). Transgenic overexpression of H-Ras^{V12} using the GFAP promoter also induced glioblastoma (Ding et al., 2001). Mice heterozygous for both *NF1* (a negative regulator of Ras) and *p53* also developed glioblastoma with moderate penetrance in some genetic backgrounds (Reilly et al., 2000). Low penetrance of astrocytoma was also observed in mice expressing a *GFAP-v-src* transgene (Weissenberger et al., 1997). Although mutations in Ras, NF1, AKT, or src have not been observed in sporadic human astrocytomas, the EGF and PDGF tyrosine kinase receptors are frequently activated (Maher et al., 2001; Reilly and Jacks, 2001;

Louis and Cavenee, 2001). One of the many downstream effects of Ras signaling is the induction of cyclin D, a mediator of cdk4-dependent pRb phosphorylation and inactivation (Sherr, 1996). Epistasis experiments combining T_{121} and activated Ras alleles will determine whether pRb is an important downstream target of Ras in the induction of astrocytoma. In *TgG(ΔZ) T_{121}* mice, tumors have not spontaneously progressed to glioblastoma, yet penetrance of the astrocytoma phenotype is 100%. It is possible that widespread effects caused by pRb inactivation in a large percentage of astrocytes preclude the development of the solid tumors associated with angiogenesis and necrosis. Mice may die with diffuse disease before mutations that facilitate solid tumor growth develop or exert a significant effect. Induction of T_{121} expression in a limited number of astrocytes through somatic introduction of Cre, as well as crosses onto a variety of mutant backgrounds, should facilitate determination of the molecular and cellular requirements for progression to glioblastoma.

Cooperating events in astrocytoma development

The long latency between widespread T_{121} expression and the development of life-threatening astrocytomas in *TgG(ΔZ)T_{121}* mice indicates that additional events could be involved. Astrocytomas are diffusely infiltrating tumors, making it difficult to assess progression by regional morphological changes. However, in screening advanced astrocytomas for the activation of specific signal transduction pathways, we showed that 72% of the astrocytomas contained regions of reduced apoptosis in which tumor cells expressed activated Akt. This result suggests that astrocytes in which the pRb pathway is inactivated are under selective pressure for deregulation of Akt, an event that may further facilitate astrocytoma development by a reduction in apoptosis. Further analysis of foci expressing activated Akt will determine whether PTEN inactivation is the molecular basis for spontaneous Akt activation. Biological changes in addition to apoptosis reduction may also be present within these regions. Some astrocytomas examined did not contain detectable regions of Akt activation. In this study, a limited number of sections from each brain were examined. Since the astrocytoma occurred essentially throughout the brain and Akt activated regions were focal, a complete assessment would require a more extensive analysis of the brain. Furthermore, as stated above, mice may die of expansive astrocytoma before significant tumor progression occurs. It is also possible that alteration of distinct pathways can lead to progression. Among the 4 p-Akt negative brains, 2 showed upregulated p-Erk1,2 expression, indicating that the MAP kinase pathway is induced, albeit at a much lower frequency than the Akt pathway. The full biological impact of these changes remains to be determined.

PTEN is inactivated in 50% of human high-grade gliomas by both LOH and epigenetic mechanisms (Reilly and Jacks, 2001; Maher et al., 2001; Louis and Cavenee, 2001). Using a genetic approach, we show here that PTEN has a role in suppressing astrocytomas initiated by pRb_f inactivation. In a *$PTEN^{+/-}$* background, *TgG(ΔZ)T_{121}* mice developed high grade astrocytoma with significantly reduced latency. This study provides direct evidence that *PTEN* mutation contributes to astrocytoma development. Even in young *TgG(ΔZ)T_{121};$PTEN^{+/-}$* mice, astrocyte apoptosis levels were reduced by about 50%, indicating a possible dose-dependent effect. PTEN haplodeficiency was recently shown to accelerate prostate cancer progression in the TRAMP model, where tumorigenesis is induced by SV40 large and small T antigens (Kwabi-Addo et al., 2001). In that case, loss of the wild-type *PTEN* allele was not detected, implicating a dosage effect. We do not yet know whether *TgG(ΔZ)T_{121};$PTEN^{+/-}$* astrocytomas undergo loss of the wild-type allele or whether haploinsufficiency of PTEN alone causes acceleration of tumor growth. Given the diffuse nature of the tumors and the possibility for epigenetic inactivation, this assessment may not be straightforward. Thus, the PTEN status will be assessed at the chromosomal, transcriptional, and protein levels. In addition, analysis of *TgG(ΔZ)T_{121}* mice harboring conditional *PTEN* null alleles will further address the role of PTEN in astrocytoma progression. For example, reduction in PTEN dosage may accelerate tumor growth via apoptosis reduction. However, if PTEN loss further reduces apoptosis and/or influences other aspects of tumor growth, selective pressure for PTEN inactivation could remain high.

In the CPE tumor model previously examined, most T_{121}-induced apoptosis was p53-dependent, and in a *$p53^{+/-}$* background, tumor progression was accelerated and correlated with spontaneous p53 inactivation (Symonds et al., 1994; Lu et al., 2001). Previously, wild-type T antigen (capable of inactivating Rb_f and p53) expressed under the GFAP promoter induced perinatal lethality (Danks et al., 1995) similar to that observed in *TgGFAP-T_{121}* founder mice, thus indicating that p53 inactivation may not alter the phenotype. Here, we show that the development of diffuse astrocytoma in *TgG(ΔZ)T_{121}* mice is indeed not accelerated in a *$p53^{+/-}$* background. Recently, oligoastrocytoma and oligodendroglioma induced by somatic delivery of PDGF was shown to be unaffected by p53 deficiency (Dai et al., 2001). In human astrocytomas, unlike many tumors, p53 mutation generally correlates with low-grade disease indicative of an early rather than a progressive event (Louis and Cavenee, 2001; Reilly and Jacks, 2001; Maher et al., 2001).

Although the diffuse astrocytic phenotype appears unaltered by p53 heterozygosity, olfactory bulb tumors uniquely develop in *TgG(ΔZ)T_{121} ;$p53^{+/-}$* mice. The cellular origin of the olfactory tumors is currently unknown; however, these tumors do not express common astrocytic markers. One possibility is that, in combination with the periventricular expansion of neural precursors observed in *TgG(ΔZ)T_{121}* mice, p53 haploinsufficiency or inactivation aberrantly influences the neuronal cells that migrate along the rostral migratory stream into the olfactory bulb. Further analysis of these tumors and the role of p53 in their development is underway.

Importantly, these studies address the cell specificity of tumorigenesis mechanisms. Together with previous studies, we show that two diverse cell types, brain epithelium and astrocytes, respond similarly to disruption of the pRb pathway. In both cases, cells proliferate aberrantly, leading to extensive apoptosis, and in both cases, this process predisposes cells to tumorigenesis. However, the events leading to tumor progression appear to be distinct in the two systems. While the epithelial tumors progress in a *$p53^{+/-}$* background and exhibit p53 inactivation (Lu et al., 2001), p53 heterozygosity does not appear to accelerate the development of diffuse anaplastic astrocytomas. In contrast, these tumors are accelerated in *$PTEN^{+/-}$* mice. In each case, tumor progression is associated with a reduction in apoptosis; however, the critical pathways involved appear to be distinct.

Experimental procedures

Transgene construction, generation, and screening of mice

To construct the GFAP-T_{121} transgene, the T_{121} coding region was removed from pLE1137 (Chen et al., 1992) and ligated to the pGfa2 Lac-1 plasmid (Dr. M. Brenner, Univ. Alabama) containing the 2.2 Kb human GFAP gene transcriptional regulatory sequences (Brenner et al., 1994). To construct the GZT_{121} transgene (Figure 1B), a 2.7 kb floxed lacZ cassette was removed from pCLLA (Drs. Y. Li and H. Varmus, Sloan Kettering), blunt ended, and ligated into the GFAP-T_{121} plasmid at the Kpn1 site (blunt ended). Both constructs were confirmed to be correct by sequencing. The EcoRV to Sal 1 transgene fragments were isolated and injected at a concentration of 4 ng/ul into fertilized eggs from BDF1 mice as previously described (Chen et al., 1992). Transgenic mice were screened using T_{121}-specific primers 2 and 3 (Figure 1B and Chen et al., 1992). *TgGZT$_{121}$* transgenic lines were maintained by crossing to nontransgenic BDF1 mice (Jackson Labs). To generate compound *TgG(ΔZ) T$_{121}$* mice, *TgGZT$_{121}$* mice were crossed to *Tg*β*-Actin Cre* mice (FVB background, provided by Drs. M. Lewondonski and G. Martin, UCSF; Lewandoski and Martin, 1997). Primer sets 2 and 3 (Chen et al., 1992), 1 and 3, and Cre-specific primers (Lewandoski and Martin, 1997) were used to screen the doubly transgenic mice and to assay for cre-mediated deletion (Lewandoski and Martin, 1997). PCR conditions for primers 2 and 3 (Chen et al., 1992) and Cre primers (Lewandoski and Martin, 1997) were as previously described. Conditions for primers 1 and 3 were 95°C 5′; 95°C 30′′, 60°C 45′′, 72°C 45′′ for 35 cycles. Primer 1: TTC ATA AAG CCC TCG CAT CCC AGG. *TgG(ΔZ) T$_{121}$* mice were crossed with *PTEN*$^{+/-}$ or *p53* $^{-/-}$ mice to introduce the haplodeficency of either gene. Screening of *p53* and *PTEN* null alleles have been described (Lu et al., 2001; Di Cristofano et al., 1998).

Southern hybridization analysis

DNA extraction and Southern blotting were performed as described (Chen et al., 1992). The T_{121}-specific probe (a Hind III fragment containing only SV40 sequences) was isolated from pGFAP-T_{121}. The control probe was a Xba1 to EcoR1 fragment from the mouse PTEN gene isolated from plasmid PTEN P1 (Di Cristofano et al., 1998) that detected a specific 8 kb Xba1 band from the PTEN locus. The T_{121} probe was hybridized first, and the filter was then stripped and hybridized with control probes. All probes were hybridized at 68°C for 16 hr.

Histology and immunodetection

Brains were removed, fixed in 4% formalin for 16–18 hr, paraffin embedded, and sectioned at 5–10 μM. Hematoxylin and eosin staining and immunohistochemistry were performed as described previously (Chen et al., 1992). For T_{121} detection, sections were pretreated in 0.1% trypsin prior to blocking. For phospho-Akt and phospho-Erk1,2 detection, sections were either pretreated with 0.1% Trypsin PBS for 20 min at 37°C or by boiling in citrus buffer (pH 6) for 10 min prior to blocking. Primary antibodies were as follows. T_{121}: a hamster ascites specific for SV40 T antigen (1:100, except in Figure 5 where it was 1:50; Chen et al., 1992); GFAP (Z0334, DAKO, rabbit at 1:100); S-100 (Z0311, DAKO, rabbit at 1:100); Tuj1 (MMS-435P, BABCO, mouse at 1:3000); PSA-NCAM (60221A, PharMingen, rat at 1:3000); PCNA (SC-7907, Santa Cruz, rabbit at 1:100); phospho-Akt $^{Ser\,473}$ (9277, Cell signaling, rabbit at 1:50); phospho-Erk1,2$^{Thr202/Tyr204}$ (9101, Cell signaling, rabbit at 1:25). Secondary antibodies were biotinylated anti-rabbit or anti-mouse (Vector Labs, 1:333) for immunohistochemistry, and FITC-conjugated anti-hamster (T_{121}, 6.5 μg/ml, Jackson ImmunoResearch Laboratories) and rhodamine-conjugated anti-rabbit for immunofluorescence (Santa Cruz, 1:300). All antibodies were diluted in 5% normal goat serum (NGS) in PBS/0.05% Tween 20.

Immunofluorescence double labeling followed the manufacturer's protocol (Jackson ImmunoResearch Laboratories). Sections were deparaffinized, treated in 0.1% trypsin in PBS at 25°C for 20 min, and blocked in 5% NGS, PBS/0.05% Tween 20 for a minimum of 1 hr. Sections were incubated with anti-T_{121} primary antibody for 1 hr, washed in PBS/0.05% Tween 20, and incubated with FITC conjugated anti-hamster secondary antibody for 30 min. After further washing, the sections were again blocked and then incubated with the second primary antibody, followed by the rhodamadine-conjugated anti-rabbit secondary antibody. Slides were stained with DAPI (10 μg/ml). Controls with single primary antibodies confirmed that secondary antibodies did not crossreact with inappropriate primary antibodies.

Primary astrocyte analysis

Brain pieces were digested in 0.05% Trypsin-EDTA (Gibco-BRL) at 37°C for 30 min, followed by repeated trituration to form single cell suspensions. Cells were plated in DMEM with N2 supplement, 10% FBS (Gibco-BRL). At passage two, 95% of the cells showed immunopositivity for GFAP (not shown). Immunoblotting followed the manufacturer's protocol (Cell Signaling). Proteins were extracted from passage two cells, separated by 10% SDS-PAGE electrophoresis and electrotransferred to PVDF membranes. Filters were incubated with primary antibody (rabbit anti phosho-Akt^{Ser473}, 9271; 1:1000) at 4°C overnight, washed extensively with TBST, incubated with HRP-conjugated goat anti-rabbit secondary antibody (1:3750), and then detected with ECL™ (Amersham). After treating with 0.2 N NaOH, the same blots were used to detect the total level of Akt and the levels of phosphorylated Erk1, 2, consecutively (rabbit anti-Akt, 9272 and anti-phospho-Erk1, 2$^{Thr202/Tyr204}$, 9101; 1:1000). All antibodies were from Cell Signaling.

Acknowledgments

We thank Eric Holland (Sloan Kettering, NY) for critical discussions and technical advice. We thank the UNC Animal Models Core for microinjection of the GZT_{121} transgene, the UNC Lineberger Comprehensive Cancer Center Histology Core for processing tissues used in this study, and the UNC Division of Laboratory Animals for excellent animal care. This work was supported by NCI grants 1 R01 CA 46283 to T.V.D. and 5 U01 CA84314 to T.V.D. and D.N.L.

Received: October 2, 2001
Revised: February 14, 2002

References

Brenner, M., Kisseberth, W.C., Su, Y., Besnard, F., and Messing, A. (1994). GFAP promoter directs astrocyte-specific expression in transgenic mice. J. Neurosci. *14*, 1030–1037.

Brunjes, P.C., and Armstrong, A.M. (1996). Apoptosis in the rostral migratory stream of the developing rat. Brain Res. Dev. Brain Res. *92*, 219–222.

Chen, J., Tobin, G., Pipas, J.M., and Van Dyke, T.A. (1992). T Antigen mutant activities in transgenic mice: roles of p53 and pRB-binding in tumorigenesis of the choroid plexus. Oncogene *7*, 1167–1175.

Cobrinik, D., Lee, M.H., Hannon, G., Mulligan, G., Bronson, R.T., Dyson, N., Harlow, E., Beach, D., Weinberg, R.A., and Jacks, T. (1996). Shared role of the pRB-related p130 and p107 proteins in limb development. Genes Dev. *10*, 1633–1644.

Dai, C., Celestino, J.C., Okada, Y., Louis, D.N., Fuller, G.N., and Holland, E.C. (2001). PDGF autocrine stimulation dedifferentiates cultured astrocytes and induces oligodendrogliomas and oligoastrocytomas from neural progenitors and astrocytes in vivo. Genes Dev. *15*, 1913–1925.

Danks, R.A., Orian, J.M., Gonzales, M.F., Tan, S.S., Alexander, B., Mikoshiba, K., and Kaye, A.H. (1995). Transformation of astrocytes in transgenic mice expressing SV40 T antigen under the transcriptional control of the glial fibrillary acidic protein promoter. Cancer Res. *55*, 4302–4310.

Datta, S.R., Brunet, A., and Greenberg, M.E. (1999). Cellular survival: a play in three Akts. Genes Dev. *13*, 2905–2927.

DeCaprio, J.A., Ludlow, J.W., Lynch, D., Furukawa, Y., Griffin, J., Piwnica Worms, H., Huang, C.M., and Livingston, D.M. (1989). The product of the retinoblastoma susceptibility gene has properties of a cell cycle regulatory element. Cell *58*, 1085–1095.

Di Cristofano, A., Pesce, B., Cordon-Cardo, C., and Pandolfi, P.P. (1998). Pten is essential for embryonic development and tumour suppression. Nat. Genet. *19*, 348–355.

Ding, H., Roncari, L., Shannon, P., Wu, X., Lau, N., Karaskova, J., Gutmann,

D.H., Squire, J.A., Nagy, A., and Guha, A. (2001). Astrocyte-specific expression of activated p21-ras results in malignant astrocytoma formation in a transgenic mouse model of human gliomas. Cancer Res. *61*, 3826–3836.

Doetsch, F., Garcia-Verdugo, J.M., and Alvarez-Buylla, A. (1997). Cellular composition and three-dimensional organization of the subventricular germinal zone in the adult mammalian brain. J. Neurosci. *17*, 5046–5061.

Dyson, N., Buchkovich, K., Whyte, P., and Harlow, E. (1989). The cellular 107K protein that binds to adenovirus E1A also associates with the large T antigens of SV40 and JC virus. Cell *58*, 249–255.

Ewen, M.E., Ludlow, J.W., Marsilio, E., DeCaprio, J.A., Millikan, R.C., Cheng, S.H., Paucha, E., and Livingston, D.M. (1989). An N-terminal transformation-governing sequence of SV40 large T antigen contributes to the binding of both p110Rb and a second cellular protein, p120. Cell *58*, 257–267.

Henson, J.W., Schnitker, B.L., Correa, K.M., von Deimling, A., Fassbender, F., Xu, H.J., Benedict, W.F., Yandell, D.W., and Louis, D.N. (1994). The retinoblastoma gene is involved in malignant progression of astrocytomas. Ann. Neurol. *36*, 714–721.

Holland, E.C., Celestino, J., Dai, C., Schaefer, L., Sawaya, R.E., and Fuller, G.N. (2000). Combined activation of Ras and Akt in neural progenitors induces glioblastoma formation in mice. Nat. Genet. *25*, 55–57.

Holland, E.C., and Varmus, H.E. (1998). Basic fibroblast growth factor induces cell migration and proliferation after glia-specific gene transfer in mice. Proc. Natl. Acad. Sci. USA *95*, 1218–1223.

Kimura, T., Budka, H., and Soler-Federsppiel, S. (1986). An immunocytochemical comparison of the glia-associated proteins glial fibrillary acidic protein (GFAP) and S-100 protein (S100P) in human brain tumors. Clin. Neuropathol. *5*, 21–27.

Kirschenbaum, B., Doetsch, F., Lois, C., and Alvarez-Buylla, A. (1999). Adult subventricular zone neuronal precursors continue to proliferate and migrate in the absence of the olfactory bulb. J. Neurosci. *19*, 2171–2180.

Kleihues, P., and Cavenee, W.K. eds. (2000). World Health Organization Classification of Tumours of the Nervous System (Lyon: WO/IARC).

Kwabi-Addo, B., Giri, D., Schmidt, K., Podsypanina, K., Parsons, R., Greenberg, N., and Ittmann, M. (2001). Haploinsufficiency of the Pten tumor suppressor gene promotes prostate cancer progression. Proc. Natl. Acad. Sci. USA *98*, 11563–11568.

Lakso, M., Pichel, J.G., Gorman, J.R., Sauer, B., Okamoto, Y., Lee, E., Alt, F.W., and Westphal, H. (1996). Efficient in vivo manipulation of mouse genomic sequences at the zygote stage. Proc. Natl. Acad. Sci. USA *93*, 5860–5865.

Lee, M.-H., Williams, B.O., Mulligan, G., Mukai, S., Bronson, R.T., Dyson, N., Harlow, E., and Jacks, T. (1996). Targeted disruption of p107: functional overlap between p107 and Rb. Genes Dev. *10*, 1621–1632.

Lewandoski, M., and Martin, G.R. (1997). Cre-mediated chromosome loss in mice. Nat. Genet. *17*, 223–225.

Louis, D.N., and Cavenee, W.K. (2001). Molecular biology of central nervous system tumors. In Cancer: Principles and Practice of Oncology. V. DeVita, S. Hellman, and S.E. Rosenberg, eds. (Philadelphia: Lippincott), pp. 2091–2100

Lu, X., Magrane, D., Louis, D., Gray, J., and Van Dyke, T.A. (2001). Selective inactivation of p53 facilitates mouse epithelial tumor progression without chromosomal instability. Mol. Cell. Biol. *21*, 6017–6030.

Maandag, A.C.R., van der Valk, M., Vlaar, M., Feltkamp, C., O'Brien, J., van Roon, M., van der Lugt, N., Berns, A., and Te Riele, H. (1994). Developmental rescue of an embryonic-lethal mutation in the retinoblastoma gene in chimeric mice. EMBO J. *13*, 4260–4268.

Maher, E.A., Furnari, F.B., Bachoo, R.M., Rowitch, D.H., Louis, D.N., Cavenee, W.K., and DePinho, R.A. (2001). Malignant glioma: genetics and biology of a grave matter. Genes Dev. *15*, 1311–1333.

Marino, S., Vooijs, M., van Der Gulden, H., Jonkers, J., and Berns, A. (2000). Induction of medulloblastomas in p53-null mutant mice by somatic inactivation of Rb in the external granular layer cells of the cerebellum. Genes Dev. *14*, 994–1004.

Podsypanina, K., Ellenson, L.H., Nemes, A., Gu, J., Tamura, M., Yamada, K.M., Cordon-Cardo, C., Catoretti, G., Fisher, P.E., and Parsons, R. (1999). Mutation of Pten/Mmac1 in mice causes neoplasia in multiple organ systems. Proc. Natl. Acad. Sci. USA *96*, 1563–1568.

Reilly, K.M., and Jacks, T. (2001). Genetically engineered mouse models of astrocytoma: GEMs in the rough? Semin. Cancer Biol. *11*, 177–191.

Reilly, K.M., Loisel, D.A., Bronson, R.T., McLaughlin, M.E., and Jacks, T. (2000). Nf1;Trp53 mutant mice develop glioblastoma with evidence of strain-specific effects. Nat. Genet. *26*, 109–113.

Robanus-Maandag, E., Dekker, M., van der Valk, M., Carrozza, M.L., Jeanny, J.C., Dannenberg, J.H., Berns, A., and Te Riele, H. (1998). p107 is a suppressor of retinoblastoma development in pRb-deficient mice. Genes Dev. *12*, 1599–1609.

Saenz-Robles, M.T., Symonds, H., Chen, J., and Van Dyke, T. (1994). Induction versus progression of brain tumor development: differential functions for the pRB- and p53-targeting domains of simian virus 40 T antigen. Mol. Cell. Biol. *14*, 2686–2698.

Sage, J., Mulligan, G.J., Attardi, L.D., Miller, A., Chen, S., Williams, B., Theodorou, E., and Jacks, T. (2000). Targeted disruption of the three Rb-related genes leads to loss of G(1) control and immortalization. Genes Dev. *14*, 3037–3050.

Schlessinger, J. (2000). Cell signaling by receptor tyrosine kinases. Cell *103*, 211–225.

Sherr, C.J. (1996). Cancer cell cycles. Science *271*, 1672–1677.

Stambolic, V., Suzuki, A., de la Pompa, J.L., Brothers, G.M., Mirtsos, C., Sasaki, T., Ruland, J., Penninger, J.M., Siderovski, D.P., and Mak, T.W. (1998). Negative regulation of PKB/Akr-Dependent cell survival by the tumor suppressor PTEN. Cell *95*, 29–39.

Stubdal, H., Zalvide, J., Campbell, K.S., Schweitzer, C., Roberts, T.M., and DeCaprio, J.A. (1997). Inactivation of pRB-related proteins p130 and p107 mediated by the J domain of simian virus 40 large T antigen. Mol. Cell. Biol. *17*, 4979–4990.

Sullivan, C.S., Trembly, J.D., Fewell, S.W., Lewis, J.A., Brodsky, J.L., and Pipas, J.M. (2000). Species-specific elements in the large T-antigen J domain are required for cellular transformation and DNA replication by simian virus 40. Mol. Cell. Biol. *20*, 5749–5757.

Suzuki, A., Pompa, J.L., Stambolic, V., Elia, A.J., Sasaki, T., Barrantes, I.B., Ho, A., Wakeham, A., Itie, A., Khoo, W., et al. (1998). High cancer susceptibility and embryonic lethality associated with mutation of the PTEN tumor suppressor gene in mice. Curr. Biol. *8*, 1169–1178.

Symonds, H., Krall, L., Remington, L., Saenz-Robles, M., Lowe, S., Jacks, T., and Van Dyke, T. (1994). p53-Dependent Apoptosis Suppresses Tumor Growth and Progression In Vivo. Cell *78*, 703–711.

Ueki, K., Ono, Y., Henson, J.W., Efird, J.T., von Deimling, A., and Louis, D.N. (1996). CDKN2/p16 or RB alterations occur in the majority of glioblastomas and are inversely correlated. Cancer Res. *56*, 150–153.

Weissenberger, J., Steinbach, J.P., Malin, G., Spada, S., Rulicke, T., and Aguzzi, A. (1997). Development and malignant progression of astrocytomas in GFAP-v-src transgenic mice. Oncogene *14*, 2005–2013.

Williams, B.O., Schmitt, E.M., Remington, L., Bronson, R.T., Albert, D.M., Weinberg, R.A., and Jacks, T. (1994). Extensive contribution of Rb-deficient cells to adult chimeric mice with limited histopathological consequences. EMBO J. *13*, 4251–4259.